Beam profiles and images from two-dimensional arrays

Chris M.W. Daft, L. Scott Smith and Matthew O'Donnell*
GE Corporate Research and Development Center
Schenectady, New York 12301

Abstract

One of the limitations of current phased array scanners is that focusing in the slice thickness direction is accomplished by a plastic lens with a fixed focus. A two-dimensional array can dynamically focus in both the slice thickness and imaging directions. In this article, comparisons are made between fixed-focus linear arrays and two-dimensional arrays using beam profiles and simulated images. Conclusions are also drawn about optimal geometries of 2d arrays.

1 Introduction

The advent of digital ultrasound scanners offers the possibility of large increases in the number of channels. In radiology, these extra channels can impact image quality by simply enlarging the aperture. In contrast, the aperture size is fixed in cardiac imaging. However, improvements in resolution and contrast can still be obtained from apertures with apodizing and dynamic focusing in the slice thickness dimension. This work describes how the performance of these arrays are simulated.

First, methods for simulation of beam profiles from acoustic radiators are reviewed. We then describe how the method chosen was made to work with imaging arrays. Beam profiles indicating the advantages of two-dimensional arrays follow. A computationally efficient way of turning these into images is described, and images from the simulation are presented. Two-dimensional arrays can be made in many shapes, so finally we consider what the most effective geometry would be.

2 Modeling acoustic radiators

To investigate the properties of two-dimensional arrays, a computationally efficient three-dimensional simulator was required. Since typical imaging pulses are short, a time domain approach seemed appropriate. Harris [1,2] has reviewed the classical methods for computing transient fields from baffled pistons: the Rayleigh integral, the King integral, the Scoch solution, and the convolution integral. The method used here interprets the field from a plane radiator as a convolution process. The pressure $p(\mathbf{r},t)$ can be expressed as the convolution of a spatial impulse response $h(\mathbf{r},t)$ and the time response of the transducer elements $E(t)$:

$$p(\mathbf{r},t) = E(t) \star h(\mathbf{r},t). \tag{1}$$

Piwakowski and Delannoy [3] have published a method for efficiently computing $h(\mathbf{r},t)$:

$$h(\mathbf{r},t) = \frac{1}{4\pi}\int_{S'} \frac{v(x',y')\alpha(\theta)\delta[t - R/c - d(x',y')]}{R} dS'. \tag{2}$$

In this equation, $h(t)$ is in units of velocity potential divided by time (Lasota *et al.* [4]). $v(x,y)$ is the normal component of the velocity of the surface of the transducer, $d(x,y)$ is the time delay at a given point, θ is the angle between the normal to dS' and the field point, $\alpha(\theta)$ is an inclination factor determined by the boundary condition, and R is the distance from dS' to the field point $\mathbf{r}$.

In [3], a discrete representation of $h(\mathbf{r},t)$ is obtained having a simple physical interpretation. Imagine the surface of the transducer divided into small areas ΔS_j. Each area emits a spherical, impulsive wave, with propagation time

$$t_j = R_j + d_j \tag{3}$$

to the field point (R_j and d_j are discretized versions of the variables R and $d(x,y)$ above). The amplitude of the impulse received at the field point is proportional to the velocity of the elemental area v_j, and also to $1/R_j$. Piwakowski and Delannoy show that if the number of elemental areas is high enough, a band-limited approximation to the acoustic field can be obtained by summing the effect of each area in the radiator. In software, a vector is set up to represent the impulse response as a function of time. The time t_j is calculated for each elemental area on the transducer, and this specifies the

*Present address: Department of Electrical Engineering and Computer Science, University of Michigan.

1051-0117/90/0000-0775 $1.00 © 1990 IEEE

point on the vector to which ΔS_j contributes. That element of the impulse response vector is incremented by $v_j \alpha / R_j$. This method of computing the integral has the virtues of speed and intuitive simplicity.

The dimensions of a physical phased array are specified in $v(x, y)$: this matrix has zero entries for positions on the integration grid outside the transducer. A constant F-number can be maintained by changing $v(x, y)$ as a function of range. The effects of apodizing, shading, and also tolerances in scanner electronics are modeled with $v(x, y)$. The simulation uses an integration grid substantially finer than the pitch of the transducer elements: this allows the response of each element to be included in the beam profile data. The "inclination factor," a consequence of operating the high-impedance transducer into a comparatively low-impedance material (tissue), is modeled by $\alpha(\theta)$ in (2).

Steering and focusing information is encoded in the delay array $d(x, y)$. In the one-dimensional case, a plastic lens in the slice thickness (y) direction is simulated by a fixed focus delay:

$$\Delta t(y) = \frac{f_y}{V_s} \left[\sqrt{1 + \frac{y^2}{f_y^2}} - 1 \right]. \qquad (4)$$

V_s is the speed of sound in tissue. In a two-dimensional array, the y focal length f_y can be varied dynamically. The beam can also be steered in the y direction if there are enough elements. In the imaging direction, the beam steering and focusing is done with the standard parabolic approximation [5]:

$$\Delta t(x) = \frac{1}{V_s}(-x \sin\theta + \frac{x^2}{2 f_x} \cos^2\theta), \qquad (5)$$

where f_x is the focal length. The effects of tap lengths in delay lines can be studied by quantizing the entries in the matrix $d(x, y)$.

Once the impulse response is calculated, the convolution of equation (1) is performed with FFTs. The result is a pressure array for each field point. The maximum absolute value is used in the beam plots.

3 Beam profiles

Figure 2 shows graphs for a 128 element one-dimensional transducer at ranges of 20 mm and 120 mm. In this case, the array is a 30 mm square, and the frequency is 3.5 MHz. The transducer performs poorly at close range. The outer elements are not used at 20 mm because the F-number is held constant at 2. This is necessary in order for the scanner delays to be computed using a parabolic approximation. But these plots only tell half the story. The y coordinate is fixed at zero for both

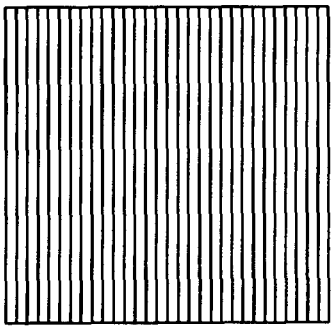

one-dimensional array
64 elements, 14 mm square

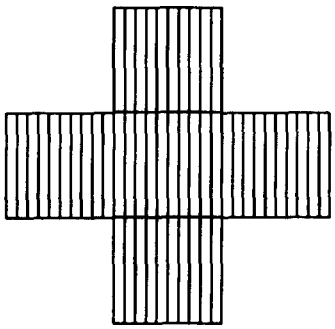

two-dimensional array
128 elements, 64 in center portion

Figure 1: Arrangement of elements in the one-dimensional and two-dimensional arrays used in simulating the images. Both arrays are 14 mm in each dimension.

plots. The real situation is made substantially worse by the inability of the one-dimensional array to maintain an adequately narrow beam width in the slice thickness dimension, both close to and far from the transducer. The voxel size increases greatly as the fixed y lens goes out of focus. A simple two-dimensional array, such as the one shown in figure 1, while inadequate for beam steering, can make a great difference to the resolution by providing dynamic focusing and apodizing. This array geometry has the advantage that the lateral cuts are no harder than for a one-dimensional array.

The one-dimensional array to be simulated in the next section has 64 elements, and is 14 mm square. The timing of the voltages applied to the elements achieves focusing and beam-steering in the normal way. The two-

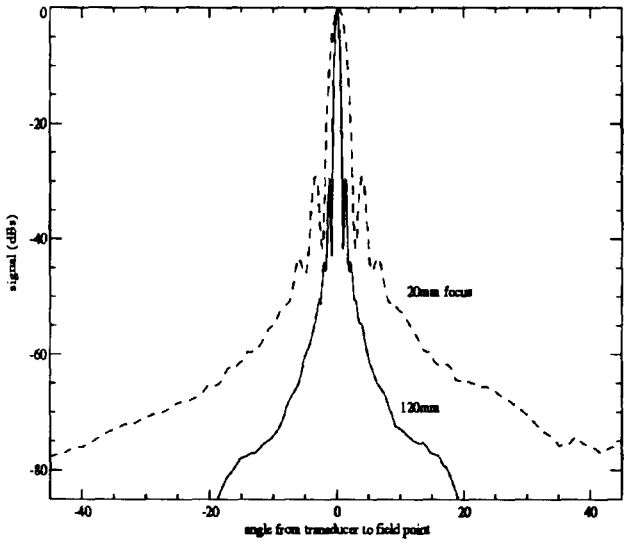

Figure 2: Beam profiles for a 128 element array at 20mm and 120mm

dimensional array has 64 elements in the central portion, and two outer banks of 32 elements. These are driven with different phasing to the central elements, which allows dynamic focusing to take place. Its longest dimension is also 14 mm, making it suitable for cardiology work. The element pitch is constant in both cases, at $\lambda/2$. In the y direction, this array is very under-sampled, and exhibits severe sidelobes, which become worse if the array is steered. Therefore, it is always operated with focusing delays only.

4 Making images

A full-scale simulation of a B-scanner is a very computationally expensive task. The following method was developed to allow the effect of the changes in beam patterns to be expressed as images using a standard workstation. This model ignores multiple scattering in tissue, and performs scanning in an idealized fashion. The beam is calculated for one focal length and and steering direction, and scanning consists of translating this pattern $p(\mathbf{r},t)$ in space. This requires only one beam calculation, and reduces image-making to a simple convolution. All images reported here use a C-scan format. Refraction of the beam in the tissue is also ignored.

Let $s(\mathbf{r})$ be the scattering function of the tissue, and $S(\mathbf{k})$ its Fourier transform. Also, define $P(\mathbf{r},\omega)$ to be the temporal transform of $p(\mathbf{r},t)$. Consider first the response of the tissue to continuous wave insonation. The effect of the transmitted sound beam is to turn the tissue into an array of sources of strength $P(\mathbf{r}-\mathbf{r}',\omega)s(\mathbf{r}')$, where $\mathbf{r}$ is the position of the transducer and $\mathbf{r}'$ is the position in the tissue. In this approximation, the receiver sensitivity is $P(\mathbf{r}-\mathbf{r}',\omega)$, so the aperture response is

$$U(\mathbf{r},\omega) = \int_V P^2(\mathbf{r}-\mathbf{r}',\omega)s(\mathbf{r}')d^3\mathbf{r}', \tag{6}$$

and the RF time waveform from the transducer using pulsed excitation is

$$u(\mathbf{r},t) = \int U(\mathbf{r},\omega)e^{j\omega t}d\omega. \tag{7}$$

If we define the self-convolution of $p(\mathbf{r},t)$ as $c(\mathbf{r},t)$:

$$c(\mathbf{r},t) = \int p(\mathbf{r},t')p(\mathbf{r},t-t')dt', \tag{8}$$

then

$$u(\mathbf{r},t) = \int c(\mathbf{r}-\mathbf{r}',t)s(\mathbf{r}')d^3\mathbf{r}'. \tag{9}$$

In (9), $u(\mathbf{r},t)$ can be calculated rapidly by taking the three-dimensional spatial transform of $c(\mathbf{r},t)$, squaring, multiplying by the three-dimensional transform of $s(\mathbf{r})$ and inverse transforming:

$$u(\mathbf{r},t) = \mathcal{F}^{-1}[C(\mathbf{k},t)S(\mathbf{k})]. \tag{10}$$

Here $C(\mathbf{k},t)$ is the three-dimensional spatial transform of $c(\mathbf{r},t)$. In practice, this only needs to be evaluated at the round-trip time for the sound pulse. An image can then be formed by taking a slice through $u(\mathbf{r},t)$, for example in the $y=0$ plane.

Figures 3 and 4 show images of a "cyst" using the one-dimensional and two-dimensional transducers of figure 1. The tissue was modeled as a collection of random scatterers, and the scattering amplitude in the cyst was 40 dB below that of the tissue. The field of view is 22 mm x 22 mm, and the cyst is 0.25 mm in the slice thickness dimension. The range was 20 mm, and the frequency of operation 3.5 MHz. The cyst is better resolved with the two-dimensional array.

The contrast-to-noise ratio, defined as

$$\frac{\overline{\log|u_{cyst}|} - \overline{log|u_{tissue}|}}{\sigma(\log|u_{tissue}|)}, \tag{11}$$

where σ denotes standard deviation, was 0.22 for the one-dimensional transducer and 3.3 for the two-dimensional transducer. This is an extreme case, but similar improvements can be expected in the 130-200 mm range with tissue structures that are thin in the slice thickness dimension.

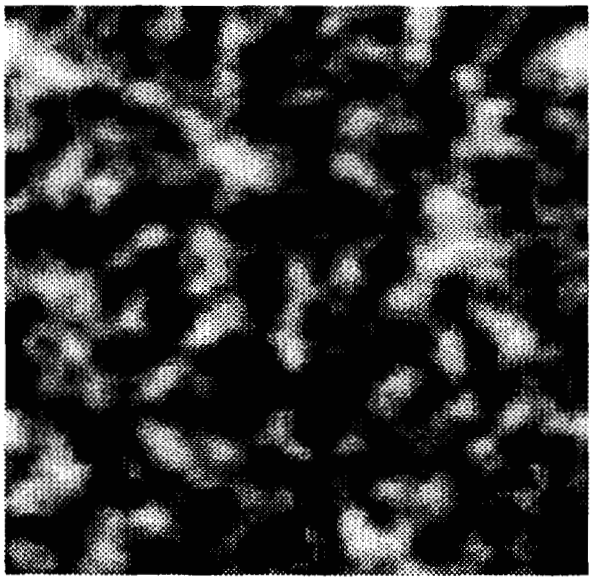

Figure 3: Image of cyst with one-dimensional transducer (22 mm field of view, 3.5MHz)

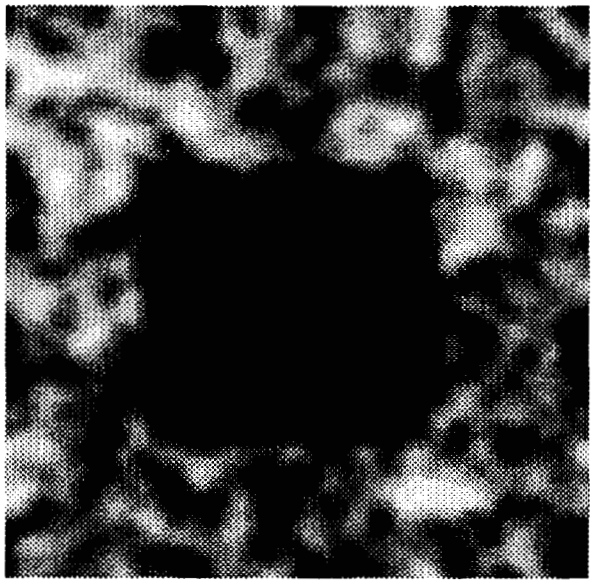

Figure 4: Image of same cyst at 3.5 MHz with two-dimensional transducer

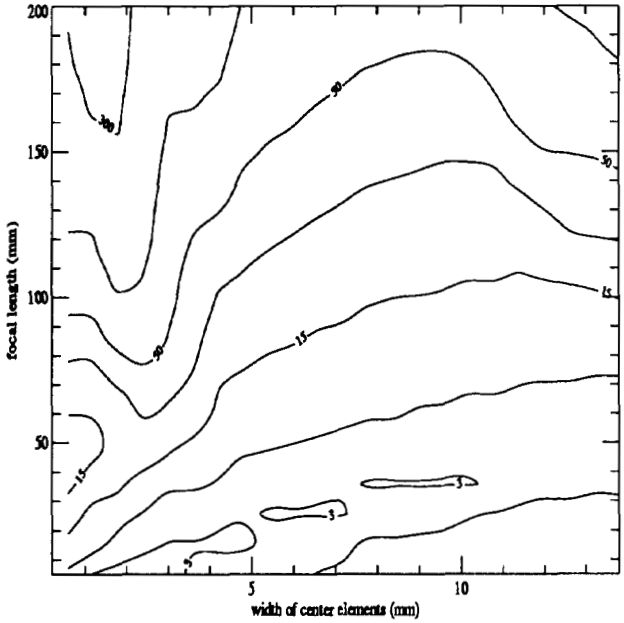

Figure 5: Contour map of resolution of 2d arrays. The 6 dB beam area (in mm^2) is plotted as a function of focal length and array geometry

5 Optimizing 2d array geometries

Given the cross-shaped design of the 2d array, what sizes should the panels of elements be? For example, what is the optimal width of the central bank of 64 elements? Beam profiles were calculated in the x and y dimensions for various widths, and the 6 dB beam area was computed. The results are plotted in Figure 5. All calculations were done with dynamic focusing in x and y; using receive-only beam patterns. The simulation also included a realistic phase slip accuracy, and a variation in sensitivity of transducer elements of $\pm$1dB.

Since the array under consideration is 14 mm square, the right-hand side of the contour map is close to a one-dimensional array. It performs poorly at large and small focal lengths. The left-hand side has two wide 32-element banks, and a thin strip of 64 elements in the center. The apodizing causes this arrangement to work well at close range. However, the beam spreads badly far from the transducer. The optimal size of the central elements can be seen to be around 8.5 - 9.0 mm. A 9 mm size corresponds to a Fresnel lens with a focal length of 92 mm: at that range, the phase change between y elements is π.

6 Conclusions

The results presented show that substantial improvements in image quality can be obtained with simple two-dimensional transducer arrays. An array with only three elements in the slice thickness direction is much better at controlling the size of the beam close to, and far from, the transducer. Potential applications would include cardiac scanning on a 128 channel system. With channel counts in the 128-512 range, it is impossible to approach Nyquist sampling in both directions and maintain an adequately large aperture. We have therefore concentrated on arrays with $\lambda/2$ sampling in x and gross undersampling in y, foregoing steering in y. When more channels are available, beam-steering in the slice thickness dimension y will become feasible. Imaging will then be possible in any scan plane, as in NMR.

7 Acknowledgements

Helpful comments on this work were provided by Wayne Rigby. Bill Leue and Carl Chalek assisted in persuading the programs to run.

8 References

1. G.R. Harris, "Review of transient field theory for a baffled planar piston," *J. Acoust. Soc. Am.* **70**(1), 10-20 (1981).

2. G.R. Harris, "Transient field of a baffled planar piston having an arbitrary vibration amplitude distribution," *J. Acoust. Soc. Am.* **70**(1), 186-204 (1981).

3. B. Piwakowski and B. Delannoy, "Method for computing spatial pulse response: Time-domain approach," *J. Acoust. Soc. Am.* **86**(6), 2422-2432 (1989).

4. H. Lasota, R. Salamon and B. Delannoy, "Acoustic diffraction analysis by the impulse method: A line impulse response approach," *J. Acoust. Soc. Am.* **76**, 280-290 (1984).

5. G.S. Kino, "Acoustic waves: Devices, imaging and analog signal processing," 229-233. Englewood Cliffs, NJ: Prentice-Hall 1987.